Effect of Foot Shape on Walking Performance of a Biped Robot Controlled by State Machine

Zhihao Zhou[1], Linqi Ye[1], Houde Liu[1(✉)], and Bin Liang[2]

[1] Tsinghua Shenzhen International Graduate School, Shenzhen 518055, China
liu.hd@sz.tsinghua.edu.cn
[2] Tsinghua University, Beijing 100084, China

Abstract. Bipedal robot is a multi-degree-of-freedom, high-dimensional, naturally unstable system. The control method based on kinematics and dynamics is complex in theory and implementation, and the control algorithm usually involves many parameters, which is difficult to design. In this paper, a control framework based on a state machine is designed to achieve stable walking of a 3D bipedal robot, which only involves 6 parameters to be designed. In terms of the structural design of biped robots, researcher's interests are mostly focused on legs, knees, and ankles, and there are few studies on the shape of the robot foot. In this paper, we build a three-dimensional biped robot model in Webots and use random searching method to find the control parameters that lead to stable walking. For the stable walking gaits, we compare the performance of five foot shapes in terms of the walking style, control efficiency, and stability. We found that the yaw angle is a key factor affecting the diversity of the robot's gait. In addition, it is found that the overall performance of the flat foot is most satisfying. The research in this paper can be helpful for the bipedal robot walking algorithm and the design of the foot shape.

Keywords: Biped robot · State machine · Foot shape

1 Introduction

The research of biped robot can be mainly divided into two fields, one is the control algorithm and the other is the structural design. Because biped robots are complex and naturally unstable, the control algorithm that enables biped robots to achieve stable walking is a primary premise. Kajita [1] proposed the LIP model and R. Blickhan [2] proposed the SLIP model. These model-based control methods reduce the order of the robot to a certain extent, but also bring errors on the model. Another common method is learning-based control. The Cassie robot from the Agility Robotics team used reinforcement learning to achieve a 5-km jog [3]. However, this method involves many parameters and the convergence is very slow. Raibert [4] proposed the control method by using a state machine, which can realize complex motion of the robot by simple feedback. This method is also used in the Altas robot.

Besides, the structural design of biped robots mostly focuses on the impact of legs, knee and ankle on motor performance [5–7]. There are few studies on the foot design,

H. Liu et al. (Eds.): ICIRA 2022, LNAI 13458, pp. 150–160, 2022.
https://doi.org/10.1007/978-3-031-13841-6_14

and most of them exist in passive walking research. Smyrli [8] studied the effects of the change in the lateral curvature of the semi-elliptical foot on the gait stability, walking speed, and energy efficiency, finding that the flat foot shape can make the gait more energy efficient. Subsequently, they expanded the foot shape to an arbitrary shape defined by a series of 2D points and established a mathematical model that verified the stability of the any convex foot geometry passive walking [9]. Kwan [10] used flat-foot and round-foot to simulate toe and heel strikes when walking, comparing the effects of foot length on walking speed, declination and centroid trajectory in long- and short-cycle gaits, respectively. And it is concluded that flat-foot and round-foot are more effective than point-foot. In terms of active robotics, Yamane [11] used the simplified model and collision dynamics to find the best walking parameters of the foot with a given shape. By comparison, they conclude that the curved feet can realize the walking speed of human beings more effectively than flat feet. Ouezdou [12] used the ADAMS physics simulation engine to compare the plate, flexible, active and hybrid flexible active feet, which differ in terms of total energy consumption and the normal contact force component, but did not change the shape of the foot. These articles are either based on passive walking robots rather than active robots, or use numerical simulation methods without physics engine simulation, or discuss them in a 2D plane rather than a 3D space. In general, there have been few studies on the impact of different foot shapes of three-dimensional, active robots on walking through physics engines.

This paper builds a three-dimensional active bipedal robot in Webots with 8 degrees of freedom that can be actively driven at each joint. The bipedal robot is controlled by a simple state machine control framework, which only involves 6 parameters. The foot shapes of Capsule, Cylinder, Box, Plane, and Flat are tested to achieve stable walking gaits by searching the control parameters randomly. Then their performance are compared in straight walking, lateral walking, in-place walking, as well as control efficiency and walking stability.

The remainder of this paper is arranged as follows. Section 2 describes the simulation model, including size, mass distribution, and joints. Section 3 introduces the control framework and control laws of the biped robot. Section 4 gives the experimental results and discussion. Conclusion is given in Sect. 5.

2 Simulation Model

2.1 Robot Model

We build a three-dimensional biped robot in the Webots software, as shown in Fig. 1a. The upper body, thigh, calf, and foot are distinguished by the hip joint, knee joint and ankle joint, respectively. The robot is 1.5 m high, 0.3 m wide, 0.13 m thick, and has a total mass of 29.84 kg. The densities of the robot are all distributed at 1000 kg/m^3, which is similar to that of humans. The mass of the robot is mainly concentrated in the upper body and thighs, and the volume and mass of each part of the robot are listed in Table 1. In order to better mimic human walking, the robot's center of mass is located in the center of the chest, at a height of about 1.02 m.

The robot has a total of eight degrees of freedom, and each leg has four degrees of freedom, all of which are active joints driven by motors. The specific distribution can

Table 1. Robot dimension and mass distribution.

Part	Dimension/m	Mass/kg
Upper body	0.3*0.13*0.43	16.77 kg
Hip	0.05*0.05*0.05	0.125
Thigh	0.13*0.14*0.34	6.188
Calf	0.04*0.04*0.04	0.06
Foot	0.05*0.14*0.01	0.07

be seen in Fig. 1b. There are two DOFs at the hip joint, which are the pitch joint and the roll joint. They are used to achieve fore-aft and side-swing of the thighs, respectively. The knee joint has a pitch joint for raising and lowering the calf. The ankle joint has a pitch joint that swings the foot up and down.

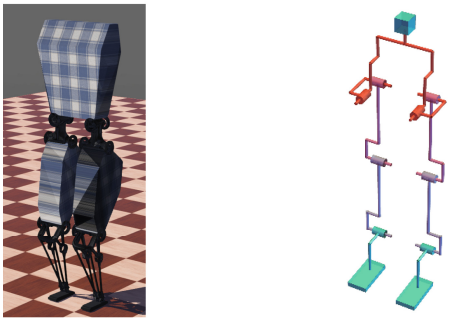

(a) (b)

Fig. 1. The biped robot studied in this paper. (a) The simulation model of the robot. (b) The degrees of freedom of the robot.

2.2 Foot Shape

In this paper, five typical foot shapes are used, namely Capsule, Cylinder, Box, Plane, and Flat, as shown in Fig. 2. The size of each foot can be seen in Table 2. With these five shapes of feet applied to the robot, we use the same control framework and control law in Sect. 3 to find out the control parameters that can run stably with different shapes of feet. We found that under the parameters that can achieve a stable gait, different shapes of the foot exhibit different walking styles. And the walking performance of different foot shapes is also different, which is discussed in Sect. 4.

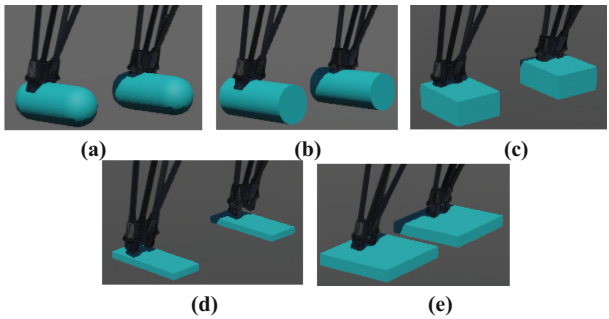

Fig. 2. Diagram of five foot shapes. (a), (b), (c), (d), (e) represent Capsule, Cylinder, Box, Plane, and Flat, respectively.

3 Control Method

3.1 Control Framework

This paper adopts the state machine control method proposed by Raibert [4], which is widely used in the control of legged robots because of its simplicity and effectiveness. As shown in Fig. 3a, the controller has four states, which are Swing stage of right leg, Landing stage of right leg, Swing stage of left leg, and Landing stage of left leg. The transition between states is triggered by two events, i.e., the step time and the swing leg touching the ground. The time of each step is set to 0.4 s, which is accumulated by the system time. The contact with the ground is judged by the touch sensors installed on the foot. The control laws for each joint in different states are given below.

There are six parameters involved in the control laws, namely $c_1, c_2, a_1, a_2, d_1, d_2, d_3, d_4$. In the simulation, their ranges are set as:

$$c_1, c_2 \in (-0.1, 0.1)$$
$$a_1 \in (-0.2, 0.2), a_2 \in (0, 1)$$
$$d_1, d_2, d_3, d_4 \in (-0.25, 0.25$$

Each time a set of parameters is randomly selected within this range. If the robot can run without falling for 10s under this parameter, then this set of parameters is called as GoodData, recorded as G_p, and the next set of parameters is taken. The random number seed is the index of cycle, so that it will change every time, thus ensuring the randomness. The control flow chart is shown in Fig. 3b.

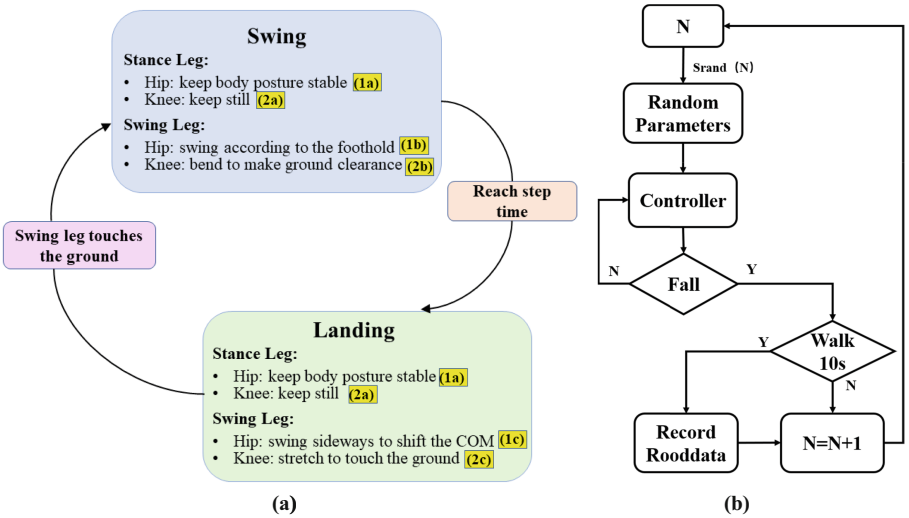

Fig. 3. The control framework. (a) The State Machine, (b) The control flow.

3.2 Low-Level Controllers

This section will discuss the control laws of the hip joint, knee joint and ankle joint respectively. Different states adopt different control laws, which are noted by a, b, c in Fig. 3. All joints adopt position control, which will not be declared in the following.

Hip Controller

- **(1a) Body posture controller**
  When a leg is the stance leg, its hip joint is used to maintain the stability of the body. The pitch joint of the hip is used to offset the pitch angle of body:

$$\theta_H^* = \theta_H + 2\theta_B \tag{1}$$

  where θ_H^* is the desired angle of the hip pitch joint, θ_H is the current angle. θ_B is the current body pitch angle.

  The roll joint of the hip is used to offset the roll angle of the body:

$$\varphi_H^* = \varphi_H - 2\varphi_B \tag{2}$$

  where φ_H^* is the desired angle of the hip roll joint, φ_H is the current angle. φ_B is the current roll angle of the body.
- **(1b) Foothold controller**
  When a leg is the swing leg and is in the Swing state, its two joints at the hip of the leg are used to achieve the desired foothold. The choice of the foothold adopts the linear feedback of the body speed. The control laws of the two joints of the hip are:

$$\begin{aligned} \theta_H^* &= 0.2 - a_2 v_F + a_1 \\ \varphi_H^* &= c_1 - 0.5 v_L \end{aligned} \tag{3}$$

where, v_L is the lateral speed of the robot,v_F is the forward speed of the robot, both of which are approximated by the difference of the position obtained by GPS.

- **(1c) Landing controller**

When a leg is the swing leg and is in the Swing state, its roll joint of the hip moves a fixed angle, which is used to shift the COM of the body:

$$\varphi_H^* = c_2 \tag{4}$$

while the pitch joint no longer moves:

$$\theta_H^* = 0 \tag{5}$$

Knee Controller

- **(2a) Stance Leg Controller**
  When a leg is the stance leg, its knee joint of the leg remains stationary to maintain upright of the leg:

$$\phi_K^* = 0 \tag{6}$$

  where ϕ_K^* is the desired angle of knee pitch joint.
- **(2b) Swing Leg Swing Controller**
  When a leg is the swing leg in the Swing state, its knee joint bends a fixed angle to make the foot off the ground:

$$\phi_K^* = -0.4 \tag{7}$$

- **(2c) Swing Leg Landing Controller**

When a leg is the swing leg in the Landing state, its knee joint is re-straighten to make the foot touch the ground and prepare for the next stance phase:

$$\phi_K^* = 0 \tag{8}$$

Ankle Controller

The ankle joint has only one pitch joint, and the control law is relatively simple, so it is not shown in Fig. 3a. Adjust the ankle to a certain angle at any stage to rotate the foot up and down.

- **(3a) Stance Leg Controller**
  When a leg is the stance leg, its ankle joint is used to maintain body stability:

$$\gamma_{sS}^* = d_1, \gamma_{sL}^* = d_3 \tag{9}$$

  where γ_{sS}^*, γ_{sL}^* are the stance leg's desired ankle angle when the other swing leg is in the Swing state and the Landing state, respectively.
- **(3b) Swing Leg Controller**

When a leg is the swing leg, its ankle joint rotates a certain angle to adjust the position of the foot to touch the ground:

$$\gamma_{wS}^* = d_2, \gamma_{wL}^* = d_4 \tag{10}$$

where γ_{wS}^*, γ_{wL}^* is the swing leg's desired ankle angle when it is in the Swing state and the Landing state, respectively.

4 Result

Based on the robot in Sect. 2.1, we use different foot shape described in Sect. 2.2, use the control method introduced in Sect. 3, run 6000 simulations on each foot shape, and finally obtain the GoodData P_G (not fall in 10s). Then using these GooDatas to control the robot, which make the robot walk stably without falling, we call them Stable Parameters, denoted as P_s (not fall in a long time). Record the total walking time of each foot shape for 6000 simulations, denoted as T (walking time before falling). The above parameters are listed in Table 2. Below we discuss the performance of these five foot shapes in straight walking, lateral walking, in-place walking, as well as control efficiency and stability.

Table 2. Simulation results of different foot shapes.

Shape	Size	P_G	P_s	T
Capsule	R = 0.03, H = 0.1	29	2	1015.234
Cylinder	R = 0.03, H = 0.14	16	4	1389.388
Box	X = 0.08, Y = 0.1, Z = 0.04	37	6	2486.380
Plane	X = 0.05, Y = 0.14, Z = 0.01	45	7	3248.828
Flat	X = 0.14, Y = 0.14, Z = 0.02	53	12	5238.526

4.1 Walking Performance

Control Efficiency

The same robot and control algorithm are used, and the random search method is used while the number of simulations is sufficient. The P_G and T generated by different shapes of the feet are different. Thus, we believe that the control efficiency of different foot shapes is different, and we define the control efficiency as follows:

$$E_i = \frac{P_{G_i}}{2\sum P_{G_i}} + \frac{T_i}{2\sum T_i} \tag{11}$$

where E_i, P_{G_i}, T_i are the control efficiency, the number of P_G, and the total duration T of the i-th foot shape, respectively. The subscripts with i all represent the parameters of the i-th foot shape, which will not be repeated below. Although some parameters have not been recorded, the difference between the walking time and 10s is very small, so the control efficiency not only considers the GoodData, but also considers the total walking time.

Stability

We define the stability of each foot shape as:

$$S_i = \frac{P_{s_i}}{\sum P_{s_i}} \tag{12}$$

From the number of P_s, it is obvious that Capsule is the most unstable one, and Flat is the most stable. Using the Capsule's P_s on Flat, it doesn't work for 10s. In the same way, if the P_s of a certain shape is applied to another, it is not possible to walk for 10s. Therefore, we can conclude that each shape has different characteristics, and its P_s is not universal.

4.2 Walking Gait

The control framework in Sect. 3 considers from the perspective of keeping the robot walking stably and not falling, and does not require the robot to achieve a specific gait such as straight walking, lateral stepping, turning, and stepping backward. We let the robot walk for ten minutes with each set of P_s using different foot shapes, and the obtained data is shown in Table 3. We found that the robot can achieve four kinds of gaits: straight walking, lateral walking, in-place walking, and backward walking with different foot shapes.

$\overline{|F|}$, $|F|_{max}$, $|F|_{min}$, are the average, maximum and minimum values of the forward distance's absolute value, respectively. $\overline{|L|}$, $|L|_{max}$, $|L|_{min}$ are the average, maximum and minimum values of lateral distance's absolute values, respectively.

Table 3. Gait data of different shapes

Shape	$\overline{\lvert F\rvert}$	$\lvert F\rvert_{max}$	$\lvert F\rvert_{min}$	$\overline{\lvert L\rvert}$	$\lvert L\rvert_{max}$	$\lvert L\rvert_{min}$
Capsule	71.99	108.29	35.68	2	65.15	5.61
Cylinder	37.9	79.39	13.69	4	9.56	5.14
Box	40.38	70.44	11.03	6	143.19	0.47
Plane	101.17	238.87	2.73	7	68.64	0.29
Flat	51.86	134.49	0.46	12	121.9	0.09

Straight Walking

The ability of straight walking is defined as:

$$\zeta_i = \frac{|F|_i}{|L|_{i\ max}} \tag{13}$$

where ζ_i is the straight walking ability of i-th foot, $|F|_i$ and $|L|_i$ are the forward and lateral walking distances under the same group of P_s.

We found that both the $\overline{|F|}$ and $|F|_{max}$ of the Plane foot are the largest. Therefore, we believe that the Plane foot has the greatest ability to walk forward. Denote the P_s of the Plane with the largest $|F|_{max}$ as P_{sF}. However, when the Plane foot walks forward, it also produces a large lateral displacement, which is a diagonal line instead of a straight line. While there is a set of P_s in the Flat foot, walking 92.79 m forward, with only 0.09 m laterally, which is a straight line. Denote this set of parameters as $P_{s\zeta}$.

Plot the IMU data of the robot when P_{sF} and $P_{s\zeta}$ are set on Plane and Flat feet, respectively, as shown in Fig. 4. It is found that the row angles of the robot are almost coincident, while the yaw angle of the Flat foot is almost 0, and the plane foot has fluctuations up and down, which is why the Flat foot can walk straighter.

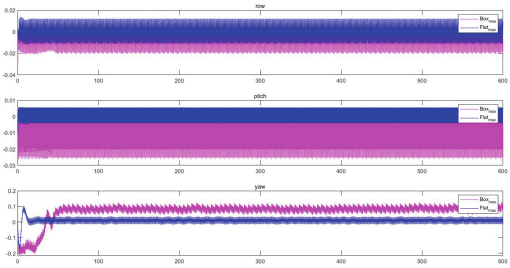

Fig. 4. IMU data for straight walking with Plane and Flat foot.

Lateral Walking

The ability of lateral walking is defined as:

$$\Gamma_i = \overline{|L|}_i + |L|_{\max i} \tag{14}$$

where Γ_i is the lateral walking ability of the i-th foot.

We found that Box foot has a significantly stronger lateral walking ability. It has a set of P_s that can walk 143.19 m laterally. Denote this set of parameters as P_{sLM}. Plot the IMU data of the robot when P_{sLM} and $P_{s\zeta}$ are set on Box and Flat feet, respectively, as shown in Fig. 5. It can be seen that the row angle and yaw angle of the Box foot are significantly larger than those of the Flat foot, which is the reason for the large lateral walking ability of the Box foot.

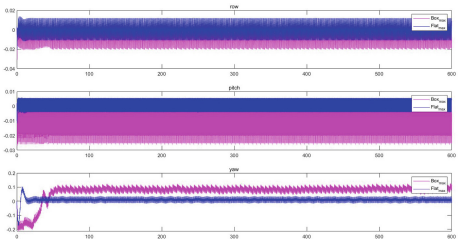

Fig. 5. IMU data for lateral walking with Box and Flat feet.

In-Place Walking

The ability of in-place walking is defined as:

$$\epsilon_i = \frac{1}{(|F| + |L|)_{min}} \tag{15}$$

where ϵ_i is the lateral walking ability of the i-th foot.

There is a set of P_s of Flat foot, which walks 4.6 m laterally and 0.49 m laterally in ten minutes, which can be approximately regarded as stepping in place. Denote this set of parameters as $P_{s\epsilon}$. Plot the IMU data of the robot when $P_{s\epsilon}$ and one random set of P_s are set on Box and Capsule foot, as shown in Fig. 6, we find that the yaw angle of $P_{s\epsilon}$ is a periodic polylines line, which is the reason why it can achieve in-place walking.

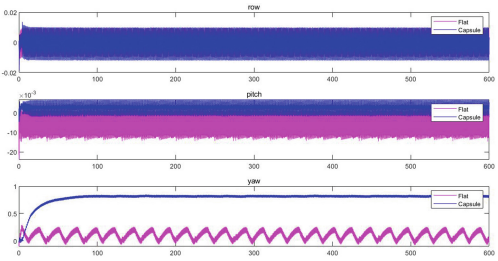

Fig. 6. IMU data for in-place walking with Capsule and Flat feet.

4.3 Discussion

According to the above analysis, we can find that the yaw angle is a key factor affecting the different walking gaits. This can also be seen from the control method. The pitch and roll angles of the robot are offset by the control law during the entire walking process to maintain stability, while the yaw angle is never controlled. Therefore, in the future, we can design different walking gaits by controlling the yaw angle of the robot.

The performance of the foot with different shapes is drawn on the radar chart as shown in Fig. 7. It can be found that the Flat feet are more prominent in straight walking, stability, and control efficiency. This can also explain why all well-known bipedal robots currently use the flat shape feet.

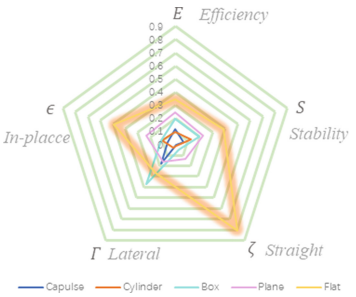

Fig. 7. Walking performance of different shapes of foot.

The video of simulation results for this article can be found in https://www.bilibili.com/video/BV1fv4y1K7nW/.

5 Conclusion

This paper builds a three-dimensional robot with eight degrees of freedom in Webots. A simple control framework based on a state machine is designed, and the whole algorithm only involves six parameters. Using the foot placement of speed feedback, the biped robot can walk continuously and stably without falling. On this basis, five shapes of feet were designed, and their performances in five aspects including control efficiency, stability, straight walking, lateral walking, and in-place walking were compared using the recorded walking data. The robot's yaw angle was found to be a key factor affecting gait diversity. In addition, the flat foot is found to be more advantageous in many aspects, which may be the reason that most biped robots choose this shape. The simple walking control law designed in this paper is helpful for bipedal walking control. What's more, the exploration in this paper can provide some explanations and references for the selection of robot feet. In the future, we will compare the performances of different feet from human experiments wearing different shapes of shoes.

Acknowledgements. This work was supported by National Natural Science Foundation of China (U1813216, 62003188), Shenzhen Science Fund for Distinguished Young Scholars (RCJC20210706091946001), and Guangdong Special Branch Plan for Young Talent with Scientific and Technological Innovation (2019TQ05Z111).

References

1. Kajita, S., et al.: Introduction to Humanoid Robotics. Introduction to Humanoid Robotics (2014)
2. Blickhan, R.: The spring-mass model for running and hopping. J. Biomech. **22**(11), 1217–1227 (1989)
3. Siekmann, J., et al.: Blind Bipedal Stair Traversal via Sim-to-Real Reinforcement Learning (2021)
4. Raibert, M.H.: Legged robots that balance. MIT press (1986)
5. Wang, K., et al.: Design and Control of SLIDER: An Ultra-lightweight, Knee-less, Low-cost Bipedal Walking Robot. In: 2020 IEEE/RSJ International Conference on Intelligent Robots and Systems (IROS) (2020)
6. Luo, G., et al.: Design and dynamic analysis of a compliant leg configuration towards the biped robot's spring-like walking. J. Intell. Rob. Syst. **104**(4), 64 (2022)
7. Yazdani, M., Salarieh, H., Foumani, M.S.: Bio-inspired decentralized architecture for walking of a 5-link biped robot with compliant knee joints. Int. J. Control Autom. Syst. **16**(6), 2935–2947 (2018). https://doi.org/10.1007/s12555-017-0578-0
8. Smyrli, A., et al.: On the effect of semielliptical foot shape on the energetic efficiency of passive bipedal gait *, pp. 6302–6307 (2019)
9. Smyrli, A., Papadopoulos, E.: A methodology for the incorporation of arbitrarily-shaped feet in passive bipedal walking dynamics. In: 2020 IEEE International Conference on Robotics and Automation (ICRA) (2020)
10. Kwan, M., Hubbard, M.: Optimal foot shape for a passive dynamic biped. J. Theor. Biol. **248**(2), 331–339 (2007)
11. Yamane, K., Trutoiu, L.: Effect of foot shape on locomotion of active biped robots. In: 2009 9th IEEE-RAS International Conference on Humanoid Robots. IEEE (2009)
12. Ouezdou, F.B., Alfayad, S., Almasri, B.: Comparison of several kinds of feet for humanoid robot, pp. 123–128 (2005)